Synthesis and Crystal Structures of the Complexes $[RhPt(\mu\text{-}H)(\mu\text{-}CO)(PEt_3)_2(PPh_3)(\eta^5\text{-}C_2B_9H_{11})]$ and $[RhPt\{\sigma\text{-}C(C_6H_4Me\text{-}4)=C(C_6H_4Me\text{-}4)H\}(CO)(PEt_3)(PPh_3)(\eta^5\text{-}C_2B_9H_{11})]$ *

Justin E. Goldberg, Judith A. K. Howard, Harald Müller, Massimino U. Pilotti, and F. Gordon A. Stone
Department of Inorganic Chemistry, The University, Bristol BS8 1TS

The reaction between $[NEt_4][Rh(CO)(PPh_3)(\eta^5\text{-}C_2B_9H_{11})]$ and $[PtCl(H)(PEt_3)_2]$ in acetone, in the presence of $TlBF_4$, affords the dimetal compound $[RhPt(\mu\text{-}H)(\mu\text{-}CO)(PEt_3)_2(PPh_3)(\eta^5\text{-}C_2B_9H_{11})]$. The structure of this complex has been established by an *X*-ray diffraction study. The Rh–Pt bond [2.734(2) Å] is bridged by a hydrido ligand [Rh–H 1.7(2), Pt–H 1.8(2) Å] and by a carbonyl group [Rh–CO 1.99(1), Pt–CO 1.99(1) Å; Rh–C–O 133(1), Pt–C–O 141(1)°]. The platinum atom carries the two PEt_3 ligands [Pt–P 2.275(4) and 2.335(4) Å], while the rhodium atom is co-ordinated by the PPh_3 molecule [Rh–P 2.257(4) Å] and the five atoms $\overline{\mathrm{CCBBB}}$ in the pentagonal face of the *nido*-$C_2B_9H_{11}$ cage. Treatment of this dimetal compound with the alkynes RC≡CR (R = Ph or C_6H_4Me-4) in tetrahydrofuran at room temperature affords the complexes $[RhPt\{\sigma\text{-}C(R)=C(R)H\}(CO)(PEt_3)(PPh_3)(\eta^5\text{-}C_2B_9H_{11})]$. An *X*-ray diffraction study on the species with R = C_6H_4Me-4 revealed the following structural features. The Rh–Pt bond [2.762(1) Å] is bridged by the $C_2B_9H_{11}$ cage such that the latter is η^5 co-ordinated to the rhodium atom while forming an exopolyhedral bond to the platinum *via* a three-centre B–H $\rightharpoonup$ Pt linkage. The boron atom involved lies in the pentagonal face of the cage ligating the rhodium, and is in the β site with respect to the two carbon atoms. The rhodium atom is co-ordinated by a PPh_3 [Rh–P 2.294(2) Å] and a CO [Rh–CO 1.845(8) Å] group. The platinum atom carries the PEt_3 ligand [Pt–P 2.221(2) Å] and a σ bonded *cis*-$C(C_6H_4Me\text{-}4)=C(C_6H_4Me\text{-}4)H$ vinyl group [Pt–C 2.036(7) Å]. N.m.r. data (^1H, $^{13}C\text{-}\{^1H\}$, $^{31}P\text{-}\{^1H\}$, and $^{11}B\text{-}\{^1H\}$) for the compounds are reported and discussed.

We have recently described reactions of the salts $[NEt_4][Rh(CO)L(\eta^5\text{-}C_2B_9H_9R_2)]$ (**1a**; L = PPh_3, R = H) and (**1b**; L = CO, R = Me) with a variety of reagents.[1] One aspect of this work has involved the synthesis of dimetal complexes in which rhodium is bonded to another transition element. For example, reactions between (**1a**) and $[Co(CO)_2(NCMe)(\eta^4\text{-}C_4Me_4)][PF_6]$, $[Rh_2(\mu\text{-}Cl)_2(CO)_4]$, and $[IrCl(CO)_2(NH_2C_6H_4Me\text{-}4)]$ afford, respectively, the dimetal compounds $[CoRh(CO)_2(PPh_3)(\eta^4\text{-}C_4Me_4)(\eta^5\text{-}C_2B_9H_{11})]$ (**2**), $[Rh_2(CO)_2(PPh_3)_2(\eta^5\text{-}C_2B_9H_{11})]$ (**3**), and $[RhIrH(\mu\text{-}\sigma\text{:}\eta^5\text{-}C_2B_9H_{10})(CO)_3(PPh_3)_2]$ (**4**).[1a] In these syntheses the carbaborane group adopts a non-spectator role, forming exopolyhedral cage bonds to the adjacent cobalt, rhodium, or iridium centres. These interactions involve either a three-centre two-electron B–H $\rightharpoonup$ M (Co or Rh) bond as in (**2**) or (**3**), or an electron-pair B–M(Ir) σ bond as in compound (**4**). Moreover, it may be noted that these exopolyhedral bonds are formed by boron atoms either α or β to the carbon atoms in the pentagonal face of the cage ligating the rhodium. In other syntheses the carbaborane ligand does not form bridge bonds. Thus treatment of the salt (**1a**) with $[AuCl(PPh_3)]$ affords the complex $[RhAu(CO)(PPh_3)_2(\eta^5\text{-}C_2B_9H_{11})]$ (**5a**) in which the carbaborane cage ligates only the rhodium centre. However, the corresponding reaction between (**1b**) and $[AuCl(PPh_3)]$ yields $[RhAu(CO)_2(PPh_3)(\eta^5\text{-}C_2B_9H_9Me_2)]$ (**5**) for which there is spectroscopic evidence for the existence in solution of two isomers (**5b**) and (**5c**).[1c] Similar behaviour involving isomers with or without exopolyhedral B–H $\rightharpoonup$ M bonds have been found in dimetal tungsten–iridium systems.[2] It is thus becoming increasingly apparent that there is a delicate balance as to whether or not the carbaborane ligand adopts a spectator or a non-spectator role in dimetal compounds.[3]

In order to extend further the chemistry of the rhodium salts (**1**) we describe herein the reaction of (**1a**) with $[PtH(Me_2CO)(PEt_3)_2][BF_4]$, the latter being generated *in situ* from $[PtCl(H)(PEt_3)_2]$.[4]

Results and Discussion

Treatment of a mixture of (**1a**) and $[PtCl(H)(PEt_3)_2]$ with $TlBF_4$ in acetone gives the red crystalline compound $[RhPt(\mu\text{-}H)(\mu\text{-}CO)(PEt_3)_2(PPh_3)(\eta^5\text{-}C_2B_9H_{11})]$ (**6**), data for which are given in Tables 1—3. The structure of this product was established by a single-crystal *X*-ray diffraction study. Selected bond distances and angles are given in Table 4 and the molecule is shown in Figure 1.

The Rh–Pt bond is bridged by a CO group [Rh–C(01) 1.99(1), Pt–C(01) 1.99(1) Å; Rh–C(01)–O(01) 133(1), Pt–C(01)–O(01) 141(1)°], and by a hydrido ligand which was located in the electron-density map, and its position refined. The Pt–H(01) separation [1.8(2) Å] is the same as that found in $[PtW(\mu\text{-}H)\{\mu\text{-}CH(C_6H_4Me\text{-}4)\}(CO)_2(PMe_3)_2(\eta\text{-}C_5H_5)]$,[5] and the Rh–H(01) distance [1.7(2) Å] is typical of that found (1.77 Å) for hydrido groups bridging rhodium–rhodium bonds in clusters.[6] The Rh–Pt bond length [2.734(2) Å] in compound (**6**) may be compared with those in the complexes $[RhPtI_3(\mu\text{-}Ph_2PCH_2AsPh_2)_2(CO)]$ [2.737(3) Å],[7] $[Rh_4Pt(\mu\text{-}CO)_2(\mu\text{-}CF_3C_2CF_3)_2(\eta\text{-}C_5H_5)_4]$ (2.679 Å),[8] and $[Rh_2Pt(\mu\text{-}CO)_2(CO)(PPh_3)(\eta\text{-}C_5Me_5)_2]$ (mean 2.655 Å).[9]

The platinum atom carries two PEt_3 groups [Pt–P(1) 2.335(4) and Pt–P(2) 2.275(4) Å, P(1)–Pt–P(2) 100.0(1)°] and, if

---

* *Supplementary data available:* see Instructions for Authors, *J. Chem. Soc., Dalton Trans.*, 1990, Issue 1, pp. xix—xxii.

Table 1. Analytical[a] and physical data for the rhodium–platinum complexes

Compound	Colour	Yield (%)	$\nu_{max.}$(CO)[b]/ cm^{-1}	Analysis (%) C	Analysis (%) H	M[c]
(**6**) [RhPt(μ-H)(μ-CO)(PEt$_3$)$_2$(PPh$_3$)(η^5-C$_2$B$_9$H$_{11}$)]	Red	51	1 764	40.5 (41.4)	6.0 (6.0)	958 (958)
(**7a**) [RhPt{σ-C(Ph)=C(Ph)H}(CO)(PEt$_3$)(PPh$_3$)(η^5-C$_2$B$_9$H$_{11}$)]	Tan	93	1 993	49.5 (48.4)	5.2 (5.2)	1 018 (1 018)
(**7b**) [RhPt{σ-C(C$_6$H$_4$Me-4)=C(C$_6$H$_4$Me-4)H}(CO)(PEt$_3$)(PPh$_3$)(η^5-C$_2$B$_9$H$_{11}$)]	Tan	96	1 992	48.2 (49.3)	5.8 (5.3)	

[a] Calculated values are given in parentheses. [b] Measured in CH$_2$Cl$_2$. [c] Molecular ion from fast atom bombardment.

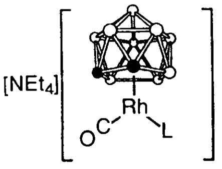

(**1a**)
(**1b**)

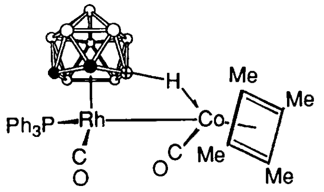

(**2**)

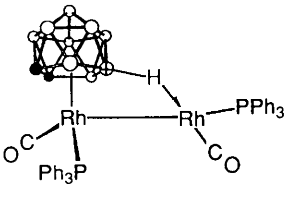

(**3**)

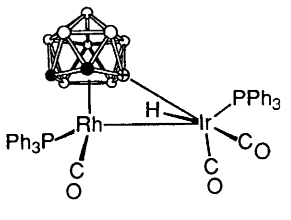

(**4**)

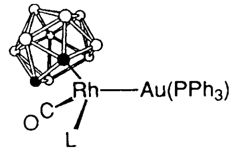

(**5a**)
(**5b**)

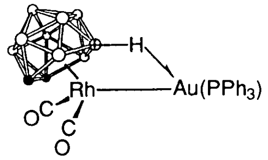

(**5c**)

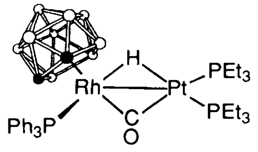

(**6**)

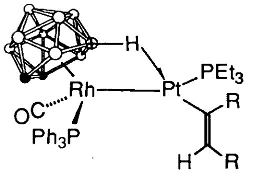

(**7a**)
(**7b**)

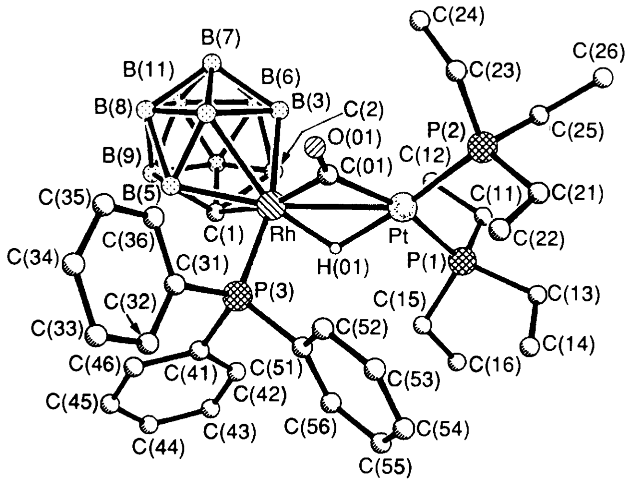

Figure 1. The molecular structure of the complex [RhPt(μ-H)(μ-CO)(PEt$_3$)$_2$(PPh$_3$)(η^5-C$_2$B$_9$H$_{11}$)] (**6**) showing the crystallographic numbering scheme

the metal–metal bond is ignored, is in a distorted square-planar environment defined by P(1), P(2), C(01), and H(01). The rhodium atom is co-ordinated by the PPh$_3$ group [Rh–P(3) 2.257(4) Å] and by the five atoms of the pentagonal $\overline{\text{CCBBB}}$ face of the *nido*-C$_2$B$_9$H$_{11}$ cage. Complex (**6**), therefore, is an example of a dimetal species in which the carbaborane ligand adopts a spectator role in the sense of not forming an exopolyhedral bond to an adjacent metal centre, in this case platinum.

The spectroscopic data for complex (**6**) are in complete agreement with the structure established by *X*-ray diffraction. The i.r. spectrum shows (Table 1) a μ-CO stretching band at 1 764 cm^{-1}. The ^{13}C-$\{^1$H$\}$ n.m.r. spectrum (Table 2) shows a CO resonance at δ 244.0 p.p.m. [*J*(RhC) 48, *J*(PC) 14 Hz]. The chemical shift and ^{103}Rh–^{13}C coupling constant values are as expected for a bridging carbonyl group.[10] The bridging hydrido ligand reveals itself in the ^{1}H n.m.r. spectrum (Table 2) by a high-field signal at δ −5.85. This resonance is split by the three non-equivalent ^{31}P nuclei and by the ^{103}Rh atom [*J*(PH) 79, 20 and 20, *J*(RhH) 12 Hz]. Moreover, ^{195}Pt–^{1}H satellite peaks are observed [*J*(PtH) 431 Hz]. The magnitude of the latter coupling is in the range found in the ^{1}H n.m.r. spectra of complexes with related molecular structures, *e.g.* [WPt(μ-H)(μ-σ:η^5-C$_2$B$_9$H$_8$Me$_2$)(CO)$_3$(PEt$_3$)$_2$] [*J*(PtH) 376 Hz][11] and [WPt{μ-CH(C$_6$H$_4$Me-4)}(CO)$_2$(PMe$_3$)$_2$(η-C$_5$H$_5$)][*J*(PtH) 509 Hz].[5] The cage CH(C$_2$B$_9$H$_{11}$) groups in complex (**6**) are non-equivalent (Figure 1) and, in agreement, two CH resonances are observed in both the ^{1}H (δ 2.36 and 2.86) and ^{13}C-$\{^1$H$\}$ (δ 45.0 and 41.7 p.p.m.) n.m.r. spectra.

The ^{11}B-$\{^1$H$\}$ n.m.r. spectrum of (**6**) (Table 3) shows six broad peaks in the range 5.3 to −26.5 p.p.m. The absence of a peak corresponding to one boron nucleus at *ca.* δ 18—36 p.p.m., as found in the spectra of compounds (**2**)—(**4**),[1a] indicates that there is no exopolyhedral bond between the cage and the platinum atom. The ^{31}P-$\{^1$H$\}$ n.m.r. spectrum displays three resonances, corresponding to the three non-equivalent phosphine ligands. The PEt$_3$ resonances at δ 20.9 and 4.9 p.p.m. show ^{195}Pt–^{31}P couplings of 4 120 and 2 600 Hz, respectively.

Table 2. Hydrogen-1 and carbon-13 n.m.r. data[a] for the rhodium–platinum complexes

Compound	^{1}H (δ)	^{13}C (δ)[b]
(**6**)	−5.85 [d of d of d of d, 1 H, μ-H, *J*(PH) 79, 20, and 20, *J*(RhH) 12, *J*(PtH) 431], 0.96 (m, 18 H, *Me*CH$_2$P), 1.93 (m, 12 H, Me*CH*$_2$P), 2.36, 2.86 [s × 2, 2 H, CH(C$_2$B$_9$H$_{11}$)], 7.32—7.67 (m, 15 H, Ph)	244.0 [d of d, μ-CO, *J*(RhC) 48, *J*(PC) 14], 135.6 [d, C^1(Ph), *J*(PC) 48], 134.2 [d, C^2(Ph), *J*(PC) 10], 130.2 [C^4(Ph)], 128.2 [d, C^3(Ph), *J*(PC) 10], 45.0, 41.7 [CH(C$_2$B$_9$H$_{11}$)], 21.0 [d, *C*H$_2$Me, *J*(PC) 26, *J*(PtC) 31], 16.6 [d, *C*H$_2$Me, *J*(PC) 31, *J*(PtC) 46], 8.7 [CH$_2$*Me*, *J*(PtC) 17], 8.3 [CH$_2$*Me*, *J*(PtC) 28]
(**7a**)	−6.59 [q, 1 H, BHPt, *J*(BH) 67], 1.01 [d of t, 9 H, *Me*CH$_2$P, *J*(PH) 18, *J*(HH) 7], 1.83 (m, 6 H, C*H*$_2$Me), 6.30 [s, 1 H, C*H*Ph, *J*(PtH) 59], 6.74—7.76 (m, 25 H, Ph)	192.0 [d of d, CO, *J*(RhC) 72, *J*(PC) 18], 150.4* [*C*(Ph)Pt], 147.0* [C^1(Ph), PtC(*Ph*)], 141.0* [C^1(Ph), C(H)*Ph*], 134.1 [d, C^2(PhP), *J*(PC) 12], 131.5 [d, C^1(PhP), *J*(PC) 27], 130.6 [C^4(PhP)], 128.4 [d, C^3(PhP), *J*(PC) 8], 125.2 [*C*(H)Ph], 45.3, 42.2 [CH(C$_2$B$_9$H$_{11}$)], 18.7 [d, *C*H$_2$Me, *J*(PC) 37, *J*(PtC) 49], 8.4 [CH$_2$*Me*, *J*(PtC) 29]
(**7b**)	−6.70 [q, 1 H, BHPt, *J*(BH) 68], 1.01 [d of t, 9 H, *Me*CH$_2$P, *J*(PH) 17, *J*(HH) 7], 1.81 (m, 6 H, C*H*$_2$Me), 2.24, 2.26 (s × 2, 6 H, Me-4), 6.20 [s, 1 H, C(*H*)C$_6$H$_4$Me-4, *J*(PtH) 60], 6.64—7.64 (m, 23 H, C$_6$H$_4$ and Ph)	192.6 [d of d, CO, *J*(RhC) 75, *J*(PC) 15], 149.3 [*C*(C$_6$H$_4$Me-4)Pt], 143.9—128.4 (C$_6$H$_4$ and Ph), 127.5 [*C*(H)C$_6$H$_4$Me-4], 45.2, 42.1 [CH(C$_2$B$_9$H$_{11}$)], 21.2 (Me-4 × 2), 18.7 [d, *C*H$_2$Me, *J*(PC) 37, *J*(PtC) 31], 8.8 [CH$_2$*Me*, *J*(PtC) 27]

[a] Chemical shifts (δ) in p.p.m., coupling constants in Hz, measurements in CD$_2$Cl$_2$ at ambient temperatures. [b] Hydrogen-1 decoupled, chemical shifts are positive to high frequency of SiMe$_4$. Peaks asterisked were unambiguously assigned *via* DEPT ^{13}C-{^{1}H} n.m.r. spectroscopy.

Table 3. Boron-11, phosphorus-31, and platinum-195 n.m.r. data[a] for the rhodium–platinum complexes

Compound	^{11}B[b] (δ)	^{31}P[c] (δ)	^{195}Pt[d] (δ)
(**6**)	5.3 (1 B), −9.2 (2 B), −14.2 (3 B), −19.8 (1 B), −21.8 (1 B), −26.5 (1 B)	44.2 [d, PPh$_3$, *J*(RhP) 157], 20.9 [s, PEt$_3$, *J*(PtP) 4 120], 4.9 [s, PEt$_3$, *J*(PtP) 2 600]	−488.5 [d of d of d, *J*(PPt) 2 600 and 4 120, *J*(RhPt) 153]
(**7a**)	[e] 26.3 [d, 1 B, B–H–Pt, *J*(BH) 67], −11.2 (2 B), −13.6 (2 B), −16.9 (2 B), −23.2 (1 B), −29.7 (1 B)	38.1 [d, PPh$_3$, *J*(RhP) 153], 19.9 [s, PEt$_3$, *J*(PtP) 4 018]	345.6 [d, *J*(PPt) 4 018]
(**7b**)	[e] 26.2 [d, B–H–Pt, *J*(BH) 70], −11.1 (2 B), −13.5 (2 B), −17.0 (2 B), −22.9 (1 B), −29.8 (1 B)	38.5 [d, PPh$_3$, *J*(RhP) 153], 20.0 [s, PEt$_3$, *J*(PtP) 4 081]	350.6 [d, *J*(PPt) 4 081]

[a] Chemical shifts (δ) in p.p.m., coupling constants in Hz, measurements in CD$_2$Cl$_2$ at ambient temperatures; all spectra are hydrogen-1 decoupled unless otherwise stated. [b] Chemical shifts are positive to high frequency of BF$_3$·Et$_2$O (external). [c] Chemical shifts are positive to high frequency of 85% H$_3$PO$_4$ (external). [d] Chemical shifts are positive to high frequency of Ξ(^{195}Pt) = 21.4 MHz. [e] Proton–boron-11 couplings measured from fully coupled ^{11}B n.m.r. spectrum.

Table 4. Selected internuclear distances (Å) and angles (°) for the complex [RhPt(μ-H)(μ-CO)(PEt$_3$)$_2$(PPh$_3$)(η^5-C$_2$B$_9$H$_{11}$)] (**6**)

Pt–Rh	2.734(2)	Pt–P(2)	2.275(4)	Pt–P(1)	2.335(4)	Pt–H(01)	1.8(2)
Pt–C(01)	1.99(1)	Rh–P(3)	2.257(4)	Rh–H(01)	1.7(2)	Rh–C(01)	1.99(1)
Rh–C(1)	2.33(1)	Rh–C(2)	2.30(1)	Rh–B(3)	2.25(2)	Rh–B(4)	2.32(2)
Rh–B(5)	2.23(2)	C(01)–O(01)	1.20(2)	C(1)–C(2)	1.58(2)	C(1)–B(5)	1.77(2)
C(1)–B(9)	1.68(3)	C(1)–B(10)	1.73(2)	C(2)–B(3)	1.75(2)	C(2)–B(6)	1.69(3)
C(2)–B(10)	1.74(2)	B(3)–B(4)	1.80(2)	B(3)–B(6)	1.80(2)	B(3)–B(7)	1.81(3)
B(4)–B(5)	1.76(2)	B(4)–B(7)	1.80(2)	B(4)–B(8)	1.73(3)	B(5)–B(8)	1.78(3)
B(5)–B(9)	1.82(2)	B(6)–B(7)	1.79(2)	B(6)–B(10)	1.76(2)	B(6)–B(11)	1.76(3)
B(7)–B(8)	1.76(2)	B(7)–B(11)	1.77(2)	B(8)–B(9)	1.78(3)	B(8)–B(11)	1.76(2)
B(9)–B(10)	1.76(2)	B(9)–B(11)	1.73(2)	B(10)–B(11)	1.69(3)		
Rh–Pt–P(2)	138.6(1)	Rh–Pt–P(1)	119.3(1)	P(2)–Pt–P(1)	100.0(1)	P(2)–Pt–H(01)	176(5)
P(1)–Pt–H(01)	84(6)	Rh–Pt–C(01)	46.7(4)	P(2)–Pt–C(01)	95.2(4)	P(1)–Pt–C(01)	164.6(4)
Pt–Rh–P(3)	100.8(1)	P(3)–Rh–H(01)	85(4)	Pt–Rh–C(01)	46.7(4)	P(3)–Rh–C(01)	90.7(3)
Pt–H(01)–Rh	102(9)	Pt–C(01)–Rh	86.7(5)	Pt–C(01)–O(01)	141(1)	Rh–C(01)–O(01)	133(1)

The larger value associated with the peak at 20.9 p.p.m. suggests that this signal is due to the PEt$_3$ ligand which is the more transoid to the Pt–Rh bond [Figure 1, P(2)–Pt–Rh 138.6(1)°]. The doublet resonance at δ 44.2 p.p.m. is readily assigned to the RhPPh$_3$ group because of the observed ^{103}Rh–^{31}P coupling (157 Hz).[1a]

The reaction between compound (**6**) and the alkynes RC≡CR (R = Ph or C$_6$H$_4$Me-4) was next investigated. It was anticipated that reaction would occur at one or other of the metal centres, and involve addition of the μ-H group to the alkyne. However, the nature of the products could not be predicted, and it was of interest to establish whether or not the C$_2$B$_9$H$_{11}$ cage adopted a spectator or non-spectator role in any product formed.

A mixture of complex (**6**) and the alkynes in thf (tetrahydrofuran) reacted slowly at room temperature to afford crystalline compounds of formulation [RhPt{σ-C(R)=C(R)H}(CO)(PEt$_3$)(PPh$_3$)(η^5-C$_2$B$_9$H$_{11}$)] (**7a**; R = Ph) and (**7b**; R = C$_6$H$_4$Me-4). Data characterising these products are given in Tables 1—3. The ^{11}B-{^{1}H} n.m.r. spectrum, discussed below, clearly showed the presence of a boron atom engaged in exopolyhedral bonding. However, in order to establish firmly

Table 5. Selected internuclear distances (Å) and angles (°) for the complex [RhPt{σ-C(C_6H_4Me-4)=C(C_6H_4Me-4)H}(CO)(PEt_3)(PPh_3)(η^5-$C_2B_9H_{11}$)] (**7b**)

Pt–Rh	2.762(1)	Pt–P(2)	2.221(2)	Pt–C(4)	2.036(7)	Pt–B(4)	2.295(7)
Rh–P(1)	2.294(2)	Rh–C(3)	1.845(8)	Rh–C(1)	2.342(6)	Rh–C(2)	2.339(6)
Rh–B(3)	2.253(8)	Rh–B(4)	2.247(7)	Rh–B(5)	2.266(9)	C(3)–O(3)	1.15(1)
C(4)–C(5)	1.34(1)	C(4)–C(40)	1.52(1)	C(5)–C(50)	1.497(8)	C(1)–C(2)	1.55(1)
C(1)–B(5)	1.74(1)	C(1)–B(7)	1.68(1)	C(1)–B(8)	1.72(1)	C(2)–B(3)	1.72(1)
C(2)–B(8)	1.72(1)	C(2)–B(9)	1.69(1)	B(3)–B(4)	1.80(1)	B(3)–B(9)	1.80(1)
B(3)–B(10)	1.81(1)	B(4)–B(5)	1.80(1)	B(4)–B(6)	1.77(1)	B(4)–B(10)	1.77(1)
B(5)–B(6)	1.81(1)	B(5)–B(7)	1.79(1)	B(6)–B(7)	1.78(1)	B(6)–B(10)	1.76(2)
B(6)–B(11)	1.78(2)	B(7)–B(8)	1.77(2)	B(7)–B(11)	1.77(2)	B(8)–B(9)	1.75(1)
B(8)–B(11)	1.75(1)	B(9)–B(10)	1.79(1)	B(9)–B(11)	1.77(2)	B(10)–B(11)	1.79(1)
B(4)–H(4)	1.32*	Pt–H(4)	1.81*	C(5)–H(50)	0.84*		
Rh–Pt–P(2)	170.3(1)	Rh–Pt–C(4)	101.9(2)	P(2)–Pt–C(4)	87.8(2)	B(4)–Pt–P(2)	118.9(2)
B(4)–Pt–C(4)	150.7(3)	B(4)–Pt–Rh	51.8(2)	B(4)–Rh–Pt	53.4(2)	Pt–Rh–P(1)	108.4(1)
Pt–Rh–C(3)	89.5(2)	P(1)–Rh–C(3)	90.1(3)	Rh–C(3)–O(3)	179.7(7)	Pt–C(4)–C(5)	120.8(7)
Pt–C(4)–C(40)	116.3(4)	C(5)–C(4)–C(40)	122.9(7)	C(4)–C(5)–C(50)	127.7(8)	Pt–B(4)–Rh	74.9(2)
B(4)–H(4)–Pt	93*	C(4)–C(5)–H(50)	104*	C(50)–C(5)–H(50)	128*		

* Parameter fixed, see text.

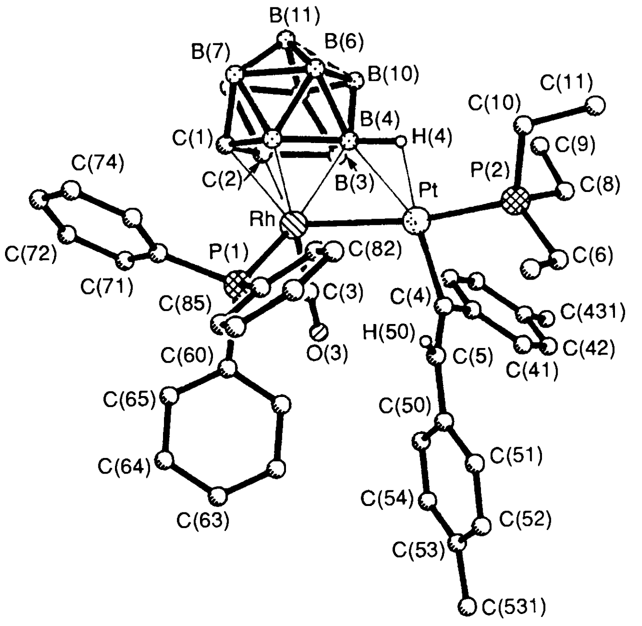

Figure 2. The molecular structure of the complex [RhPt{σ-C(C_6H_4-Me-4)=C(C_6H_4Me-4)H}(CO)(PEt_3)(PPh_3)(η^5-$C_2B_9H_{11}$)] (**7b**), showing the crystallographic numbering scheme

the structure of these species, an *X*-ray diffraction study was carried out on (**7b**). The results are summarised in Table 5, and the structure is shown in Figure 2.

The Rh–Pt bond [2.762(1) Å] is bridged by the $C_2B_9H_{11}$ cage such that the latter is η^5 co-ordinated to the rhodium atom while forming an exopolyhedral three-centre two-electron B–H ⇀ Pt bond. The latter involves the boron atom [B(4)] in the face of the cage which is in the β position with respect to the two CH groups [B(4)–Pt 2.295(7), B(4)–Rh 2.247(7) Å]. In this respect the bonding of the cage to the dimetal centre is similar to that found in compound (**3**). *X*-Ray crystallographic and n.m.r. studies carried out on several dimetal compounds have shown that exopolyhedral B–H ⇀ M bonds commonly occur. Moreover, the BH fragments involved in these bonds can be in either the α or the β sites with respect to the carbons in the $\overline{\text{CCBBB}}$ face of the ligand. In solution dynamic behaviour may occur involving exchange between the two sites.[2]

Of particular interest in the structure of (**7b**) is the presence of the *cis*-C(C_6H_4Me-4)=C(C_6H_4Me-4)H vinyl group σ bonded to the platinum atom. This group is evidently formed by addition of the hydrido ligand in the precursor (**6**) to the alkyne. The σ vinyl group in (**6**) is unusual since if such groups are present in dimetal species they are generally σ bonded to one metal centre and η^2 complexed to the other, as in [WPt{μ-C(C_6H_4Me-4)=CH_2}$(CO)_2(PMe_3)_2$(η-C_5H_5)].[12] The Pt–C(C_6H_4Me-4) [2.02(1) Å] and C=C [1.43(2) Å] distances in the latter may be compared with corresponding bond lengths in (**7b**) [Pt–C(4) 2.036(7) and C(4)–C(5) 1.34(1) Å]. The C=C distance is shorter than that in the tungsten–platinum species, as expected, since in the latter it is π complexed to the tungsten.

The rhodium atom in (**7b**) is co-ordinated by the PPh_3 ligand [Rh–P(1) 2.294(2) Å] and the carbonyl group [Rh–C(3) 1.845(8) Å, Rh–C(3)–O(3) 179.7(7)°], and also by the five atoms in the $\overline{\text{CCBBB}}$ face of the *nido*-icosahedral $C_2B_9H_{11}$ fragment. The platinum atom as expected carries the PEt_3 group [Pt–P 2.221(2) Å], which lies transoid to the metal–metal bond [P(2)–Pt–Rh 170.3(1) Å].

Having established the structure of (**7b**), and by inference that of (**7a**), since they are clearly analogues, it is possible to readily interpret their spectroscopic properties. Both compounds show a single terminal carbonyl group band in their i.r. spectra (Table 1). In the ^1H n.m.r. spectra of both complexes (Table 2) the B–H ⇀ Pt linkage is revealed by a quartet signal at high field: (**7a**), δ −6.59, *J*(BH) 67 Hz; (**7b**), δ −6.70, *J*(BH) 68 Hz. In agreement with the ^1H data, the fully coupled ^{11}B n.m.r. spectra (Table 3) show doublet resonances at δ 26.3, (**7a**), and 26.2 p.p.m., (**7b**), with ^1H–^{11}B couplings of *ca.* 70 Hz. The corresponding data for complex (**3**) are: ^1H n.m.r., δ −5.8, *J*(BH) 80 Hz; ^{11}B-{^1H} n.m.r., δ 18.7 p.p.m.[14]

In the ^{13}C-{^1H} n.m.r. spectra of (**7a**) and (**7b**) there are resonances for the terminal CO groups at δ 192.0 and 192.6 p.p.m., respectively. Moreover, these signals show the expected ^{103}Rh–^{13}C and ^{31}P–^{13}C couplings.[1] In each spectrum the non-equivalent cage CH groups display two resonances: (**7a**), δ 42.2 and 45.3; (**7b**), δ 42.1 and 45.2 p.p.m. Assignment of the peaks due to the *C*(R)=*C*(R)H nuclei of the vinyl groups was accomplished using distortionless enhancement of polarisation transfer (DEPT) techniques. The ^{31}P-{^1H} n.m.r. spectra (Table 3) show two resonances, and these signals are readily assigned to the $RhPPh_3$ and $PtPEt_3$ groups on the basis of the observed ^{103}Rh–^{31}P and ^{195}Pt–^{31}P couplings. Thus for compound (**7a**) the resonance at δ 38.1 p.p.m. is a doublet [*J*(RhP) 153 Hz],

Table 6. Data[a] for crystal structure analysis of compounds (**6**) and (**7b**)

	(**6**)	(**7b**)
Formula	$C_{33}H_{57}B_9OP_3PtRh$	$C_{43}H_{56}B_9OP_2PtRh$
M	958.0	1 046.1
a/Å	10.389(6)	11.958(3)
b/Å	11.506(5)	14.106(3)
c/Å	18.742(5)	16.593(3)
α/°	101.23(3)	72.84(2)
β/°	93.78(3)	72.08(2)
γ/°	113.23(3)	70.19(2)
U/Å^3	1 994(2)	2 448(1)
D_c/g cm^{-3}	1.57	1.42
F(000)	952	1 013
μ(Mo-K_α)/cm^{-1}	40.9	33.0
T/K	190	298
Approx. crystal size (mm)	0.80 × 0.80 × 0.28	0.40 × 0.30 × 0.20
No. of unique data	[b]4 684	8 648
No. of data used	4 321	6 690
Criterion for data used, n in $F \geqslant n\sigma(F)$	2.0	4.0
Weighting scheme: g in $w^{-1} = [\sigma_c^2(F_o) + g\|F_o\|^2]$[c]	0.000 26	0.0010
S[c]	2.68	1.01
$R(R')$[c]	5.8 (5.5)	3.7 (3.7)
Largest final electron-density difference features (e Å^{-3})	+1.8, −2.0	−0.90, −0.62

[a] Siemens R3m/V diffractometer, using Mo-K_α radiation (graphite monochromator, $\bar{\lambda} = 0.710\ 73$ Å), operating in a θ–2θ scan mode in the range $2.9 \leqslant 2\theta \leqslant 50°$. Details in common: crystal system, triclinic; habit, prisms; colour, red; space group $P\bar{1}$; $Z = 2$. [b] For compound (**6**) the data collected over the range $40 \leqslant 2\theta \leqslant 50°$ were incomplete to the extent of *ca.* 1 500 reflections, due to failure of the low-temperature unit. [c] $R = \Sigma||F_o| - |F_c||/\Sigma|F_o|$; $R' = \Sigma w^{\frac{1}{2}}||F_o| - |F_c||/\Sigma w^{\frac{1}{2}}|F_o|$; $S = [\Sigma w\Delta^2/(N_{obs.}-N_{var.})]^{\frac{1}{2}}$ where $\Delta = |F_o| - |F_c|$; $w^{-1} = [\sigma_c^2(F_o) + gF^2]$, $\sigma_c^2(F_o)$ = variance in F_o due to counting statistics; g was chosen so as to minimise variation in $\Sigma w(|F_o| - |F_c|)^2$ with $|F_o|$.

while that at 19.9 p.p.m. is a singlet with ^{195}Pt satellite peaks [J(PtP) 4 018 Hz].

The compounds (**6**) and (**7**) described in this paper provide further examples of the versatile behaviour of the η^5-$C_2B_9H_{11}$ ligand. In complex (**6**) the cage functions formally as a four-electron donor to the rhodium centre, and together with the other ligands present enables the Rh and Pt atoms to acquire 18- and 16-electron valence shells, respectively. In the complexes (**7**) the presence of the exopolyhedral B–H $\rightharpoonup$ Pt bonds allows the respective Pt atoms to attain 16-electron configurations. In this bonding mode the $C_2B_9H_{11}$ *nido*-icosahedral fragment formally contributes six electrons to the dimetal fragment.

Experimental

Light petroleum refers to that fraction of b.p. 40—60 °C. Experiments were carried out using Schlenk-tube techniques, under a dry oxygen-free atmosphere. Alumina (Brockman activity II) and silica gel (Fluka, Kieselgel 70—230 mesh) were employed in the chromatography (2 × 15 cm columns). The complex $[NEt_4][Rh(CO)(PPh_3)(\eta^5\text{-}C_2B_9H_{11})]$ was synthesised as described in the literature,[13] and the reagent $[PtH(Me_2CO)(PEt_3)_2][BF_4]$ was prepared *in situ* from $[PtCl(H)(PEt_3)_2]$.[4] The instrumentation used for the n.m.r. studies has been reported previously.[2] Infrared spectra were measured with a Perkin-Elmer FT1600 spectrophotometer. Analytical and other data for complexes (**6**) and (**7**) are given in Table 1.

Synthesis of the Complex $[RhPt(\mu\text{-}H)(\mu\text{-}CO)(PEt_3)_2(PPh_3)(\eta^5\text{-}C_2B_9H_{11})]$.—A mixture of complex (**1a**) (0.42 g, 0.64 mmol), $[PtCl(H)(PEt_3)_2]$ (0.30 g, 0.64 mmol), and $TlBF_4$ (0.21 g, 0.72 mmol) in acetone (75 cm^3) was stirred at room temperature for 24 h, after which treatment a deep red solution and a white precipitate of TlCl formed. The mixture was filtered through a Celite plug (*ca.* 3 cm), solvent was removed *in vacuo*, and the residue was dissolved in CH_2Cl_2–light petroleum (8 cm^3, 3:2) and chromatographed on an alumina column. Elution with the same solvent mixture removed initially a yellow-green fraction containing an inseparable mixture of minor products. This was followed by an orange band, containing the major product, which was eluted with CH_2Cl_2–light petroleum (4:1). Removal of solvent *in vacuo* afforded a red solid which was crystallised from CH_2Cl_2–light petroleum (*ca.* 40 cm^3, 1:2) at −78 °C to yield red *crystals* of $[RhPt(\mu\text{-}H)(\mu\text{-}CO)(PEt_3)_2(PPh_3)(\eta^5\text{-}C_2B_9H_{11})]$ (**6**) (0.32 g), dried *in vacuo*.

Reactions with Alkynes.—(*i*) A mixture of complex (**6**) (0.10 g, 0.10 mmol) and C_2Ph_2 (0.042 g, 0.22 mmol) in thf (15 cm^3) was stirred at room temperature for *ca.* 3 d, after which an i.r. spectrum revealed that the reaction was complete. Solvent was removed *in vacuo* from the dark brown solution, and the residue was dissolved in CH_2Cl_2–light petroleum (5 cm^3, 2:3) and chromatographed on Kieselgel. Elution with the same solvent mixture yielded a bright yellow eluate. Removal of solvent *in vacuo* gave a yellow-brown solid which was crystallised at 0 °C from CH_2Cl_2–light petroleum (*ca.* 10 cm^3, 1:20) to afford light tan *crystals of* $[RhPt\{\sigma\text{-}C(Ph)=C(Ph)H\}(CO)(PEt_3)(PPh_3)(\eta^5\text{-}C_2B_9H_{11})]$ (**7a**) (0.095 g), dried *in vacuo*.

(*ii*) Using a similar procedure, compound (**6**) (0.10 g, 0.10 mmol) and $C_2(C_6H_4Me\text{-}4)_2$ (0.041 g, 0.20 mmol) in thf (15 cm^3) afforded tan *crystals* of $[RhPt\{\sigma\text{-}C(C_6H_4Me\text{-}4)=C(C_6H_4\text{-}Me\text{-}4)H\}(CO)(PEt_3)(PPh_3)(\eta^5\text{-}C_2B_9H_{11})]$ (**7b**) (0.10 g).

Crystal Structure Determinations.—Data for the two complexes are given in Table 6. Intensity data were corrected for Lorentz, polarisation, and *X*-ray absorption effects. For (**6**) an analytical absorption correction was applied, using well developed faces <100>, <010>, and <001>. For (**7b**) an empirical method based upon azimuthal scan data was employed.[14] The structures were solved by first locating the metal atoms by direct methods, with all other non-hydrogen atoms being found subsequently in difference-Fourier maps. Refinements were carried out by full-matrix least-squares techniques on a DEC micro-Vax II computer with the SHELXTL PLUS system of programs.[14] Carbon atoms were distinguished from boron by initially treating all cage atoms as borons until sufficient data became available to allow a distinction to be made on the basis of thermal parameters and atom separations (C–C usually ⩽ 1.65, B–B usually ⩾ 1.70 Å).

The hydrogen atoms H(01) [complex (**6**)], H(4) and H(50) [complex (**7b**)] were located in the difference-Fourier maps in the intermediate stages of refinement. The atoms H(4) and H(50) were refined initially and then fixed, whereas H(01) was fully refined. All other hydrogen atoms were generated in calculated positions (C–H 0.96; B–H 1.10 Å using BHGEN[15]) with fixed isotropic parameters [C*H*, $U_{iso} = 0.08$; B*H*, $U_{iso} = 1.2\ U_{iso}(B)$]. All non-hydrogen atoms were refined with anisotropic thermal parameters. Atomic scattering factors and corrections for anomalous dispersion were taken from ref. 16. Atom co-ordinates for (**6**) and (**7b**) are listed in Tables 7 and 8, respectively. Complex (**7b**) crystallised with solvent molecules [C(01)—C(07) of Table 8], which were shown to be highly disordered within cavities in the crystal lattice. The nature of the solvent molecules could not be clearly identified, the complex having been crystallised from a mixture of CH_2Cl_2 and light petroleum. However, the electron-density maxima located in

Table 7. Atomic positional parameters (fractional co-ordinates × 10^4) for compound (**6**) with estimated standard deviations in parentheses

Atom	*x*	*y*	*z*	Atom	*x*	*y*	*z*
Pt	4 964(1)	1 510(1)	7 375(1)	C(36)	3 894(15)	−3 576(11)	6 268(6)
Rh	4 930(1)	−686(1)	7 744(1)	C(41)	1 689(15)	−2 899(11)	7 839(6)
P(3)	2 751(4)	−2 163(3)	7 174(2)	C(42)	1 403(16)	−2 089(13)	8 394(6)
P(2)	6 037(4)	2 836(3)	6 635(2)	C(43)	623(17)	−2 605(14)	8 911(7)
P(1)	4 211(4)	2 873(3)	8 158(2)	C(44)	159(18)	−3 917(15)	8 906(8)
O(01)	5 549(12)	−425(8)	6 263(5)	C(45)	482(17)	−4 705(14)	8 367(8)
C(01)	5 293(15)	−3(11)	6 845(7)	C(46)	1 231(16)	−4 209(12)	7 827(6)
H(01)	4 124(181)	372(142)	7 907(77)	C(51)	1 646(15)	−1 593(10)	6 659(6)
C(11)	5 554(17)	4 150(11)	8 888(6)	C(52)	1 866(16)	−1 531(12)	5 937(6)
C(12)	6 454(17)	3 654(13)	9 318(7)	C(53)	1 050(18)	−1 133(13)	5 520(7)
C(13)	3 418(16)	3 744(11)	7 698(7)	C(54)	0(18)	−826(13)	5 787(8)
C(14)	2 114(17)	2 827(14)	7 126(8)	C(55)	−214(16)	−865(12)	6 512(7)
C(15)	2 829(16)	1 984(11)	8 636(7)	C(56)	606(16)	−1 270(12)	6 937(7)
C(16)	2 144(19)	2 760(15)	9 108(9)	C(1)	5 136(15)	−1 210(10)	8 875(6)
C(21)	4 865(18)	2 961(13)	5 922(7)	C(2)	6 198(17)	233(11)	8 913(6)
C(22)	3 882(18)	1 659(14)	5 423(8)	B(3)	7 247(18)	332(12)	8 217(7)
C(23)	7 248(16)	2 382(12)	6 098(6)	B(4)	6 783(19)	−1 325(13)	7 727(8)
C(24)	8 504(16)	2 403(13)	6 581(7)	B(5)	5 336(19)	−2 259(12)	8 111(7)
C(25)	7 069(17)	4 497(11)	7 137(7)	B(6)	7 899(18)	498(15)	9 162(8)
C(26)	7 735(18)	5 509(12)	6 697(8)	B(7)	8 300(18)	−514(15)	8 443(8)
C(31)	2 667(17)	−3 523(11)	6 458(7)	B(8)	7 072(20)	−2 129(15)	8 369(8)
C(32)	1 356(16)	−4 467(11)	6 068(6)	B(9)	5 987(20)	−2 115(14)	9 061(8)
C(33)	1 299(19)	−5 464(13)	5 497(7)	B(10)	6 569(21)	−505(15)	9 580(8)
C(34)	2 550(19)	−5 499(12)	5 317(7)	B(11)	7 755(21)	−1 045(15)	9 240(8)
C(35)	3 831(18)	−4 564(11)	5 683(7)				

Table 8. Atomic positional parameters (fractional co-ordinates × 10^4) for compound (**7b**) with estimated standard deviations in parentheses

Atom	*x*	*y*	*z*	Atom	*x*	*y*	*z*
Pt	1 181(1)	1 256(1)	1 671(1)	C(64)	−3 962	268	5 434
Rh	865(1)	−399(1)	3 026(1)	C(65)	−2 998	−296	4 888
P(1)	−1 127(2)	−442(1)	3 343(1)	C(70)	−1 115	−1 795	3 754
P(2)	1 596(2)	2 388(1)	444(1)	C(71)	−841(4)	−2 288(3)	4 560(3)
C(3)	445(7)	441(5)	3 800(4)	C(72)	−744	−3 340	4 869
O(3)	183(5)	968(4)	4 280(3)	C(73)	−921	−3 897	4 372
C(4)	308(7)	2 470(5)	2 265(4)	C(74)	−1 195	−3 403	3 566
C(5)	−911(7)	2 863(5)	2 396(4)	C(75)	−1 291	−2 352	3 257
C(6)	359(9)	3 498(7)	170(6)	C(80)	−1 937	−18	2 480
C(7)	−655(12)	3 216(12)	−5(9)	C(81)	−1 385(3)	372(4)	1 628(3)
C(8)	2 786(9)	2 945(7)	413(6)	C(82)	−2 016	666	974
C(9)	3 929(9)	2 136(9)	596(7)	C(83)	−3 200	573	1 172
C(10)	2 185(9)	1 773(7)	−478(5)	C(84)	−3 752	183	2 023
C(11)	2 488(11)	2 482(9)	−1 368(6)	C(85)	−3 121	−112	2 677
C(40)	1 108	2 900	2 531	C(1)	1 816(6)	−2 154(5)	3 049(4)
C(41)	883(4)	3 967(3)	2 384(3)	C(2)	2 623(6)	−1 690(5)	3 313(4)
C(42)	1 632	4 381	2 600	B(3)	2 894(7)	−594(5)	2 579(5)
C(43)	2 607	3 728	2 962	B(4)	2 178(7)	−460(6)	1 728(5)
C(44)	2 832	2 661	3 109	B(5)	1 384(7)	−1 448(6)	2 089(5)
C(45)	2 083	2 247	2 894	B(6)	2 843(7)	−1 600(6)	1 316(5)
C(431)	3 373(13)	4 165(10)	3 255(7)	B(7)	2 532(8)	−2 659(6)	2 169(5)
C(50)	−1 714	3 630	2 938	B(8)	3 332(7)	−2 825(6)	2 962(5)
C(51)	−2 642(5)	4 431(4)	2 619(3)	B(9)	4 027(7)	−1 824(7)	2 640(6)
C(52)	−3 416	5 142	3 121	B(10)	3 762(8)	−1 071(6)	1 608(5)
C(53)	−3 262	5 052	3 943	B(11)	3 996(8)	−2 443(7)	1 867(5)
C(54)	−2 334	4 251	4 262	C(01)*	5 590(116)	4 789(103)	16(89)
C(55)	−1 560	3 540	3 760	C(02)*	5 550(109)	4 647(87)	590(74)
C(531)	−4 076(9)	5 859(7)	4 470(7)	C(03)*	5 791(44)	4 511(44)	548(35)
C(60)	−2 298	212	4 161	C(04)*	4 389(67)	5 423(50)	452(42)
C(61)	−2 563(5)	1 285(3)	3 980(3)	C(05)*	5 239(55)	4 933(45)	1 007(37)
C(62)	−3 527	1 850	4 526	C(06)*	6 019(42)	3 151(35)	1 615(29)
C(63)	−4 227	1 341	5 253	C(07)*	5 783(47)	3 861(42)	1 008(34)

* Solvent atom, see text.

the difference-Fourier synthesis could be refined as one-quarter carbon atoms. The crystal data [Table 6, *M*, D_c, *F*(000), and μ(Mo-K_α)] do not include the solvent. Inclusion of these disordered solvent molecules into the model was found to reduce the final $R(R')$ by only 1%.

Additional material available from the Cambridge Crystallographic Data Centre comprises H-atom co-ordinates, thermal parameters, and remaining bond distances and angles.

Acknowledgements

We thank the S.E.R.C. for research studentships (to J. E. G. and M. U. P.).

References

1 (*a*) J. R. Fernandez, G. F. Helm, J. A. K. Howard, M. U. Pilotti, and F. G. A. Stone, *J. Chem. Soc., Dalton Trans.*, 1990, 1747; (*b*) H. F. Dare, J. A. K. Howard, M. U. Pilotti, F. G. A. Stone, and J. Szameitat, *ibid.*, p. 2263; (*c*) N. Carr, M. C. Gimeno, J. E. Goldberg, M. U. Pilotti, F. G. A. Stone, and Isil Topaloğlu, *ibid.*, p. 2253; (*d*) M. U. Pilotti and F. G. A. Stone, *ibid.*, p. 2625.

2 J. C. Jeffery, M. A. Ruiz, P. Sherwood, and F. G. A. Stone, *J. Chem. Soc., Dalton Trans.*, 1989, 1845.

3 F. G. A. Stone, *Adv. Organomet. Chem.*, 1990, **31**, 53.

4 D. Afzal, P. G. Lenhert, and C. M. Lukehart, *J. Am. Chem. Soc.*, 1984, **106**, 3050.

5 J. C. Jeffery, I. Moore, and F. G. A. Stone, *J. Chem. Soc., Dalton Trans.*, 1984, 1571.

6 A. G. Orpen, L. Brammer, F. H. Allen, O. Kennard, D. G. Watson, and R. Taylor, *J. Chem. Soc., Dalton Trans.*, 1989, S1.

7 A. L. Balch, R. R. Guimerans, J. Lineham, M. M. Olmstead, and D. E. Oram, *Organometallics*, 1985, **4**, 1443.

8 R. S. Dickson, G. D. Fallon, M. J. Liddell, B. W. Skeleton, and A. H. White, *J. Organomet. Chem.*, 1987, **327**, C51.

9 M. Green, R. M. Mills, G. N. Pain, F. G. A. Stone, and P. Woodward, *J. Chem. Soc., Dalton Trans.*, 1982, 1309.

10 M. Green, R. M. Mills, G. Pain, F. G. A. Stone, and P. Woodward, *J. Chem. Soc., Dalton Trans.*, 1982, 1321; M. Green, J. A. K. Howard, G. N. Pain, and F. G. A. Stone, *ibid.*, p. 1327.

11 M. J. Attfield, J. A. K. Howard, A. N. de M. Jelfs, C. M. Nunn, and F. G. A. Stone, *J. Chem. Soc., Dalton Trans.*, 1987, 2219.

12 M. R. Awang, R. D. Barr, M. Green, J. A. K. Howard, T. B. Marder, and F. G. A. Stone, *J. Chem. Soc., Dalton Trans.*, 1985, 2009.

13 J. A. Walker, C. B. Knobler, and M. F. Hawthorne, *Inorg. Chem.*, 1985, **24**, 2688.

14 G. M. Sheldrick, SHELXTL PLUS, programs for use with the Nicolet *X*-Ray System, Revision 5.1, 1985.

15 P. Sherwood, BHGEN, a program for the calculation of idealised H-atom positions for a *nido*-icosahedral carbaborane fragment, University of Bristol, 1986.

16 'International Tables for *X*-Ray Crystallography,' Kynoch Press, Birmingham, 1974, vol. 4.

Received 15*th March* 1990; *Paper* 0/01159B